Interplay of microRNAs, transcription factors and target genes: linking dynamic expression changes to function

Petr V. Nazarov[1], Susanne E. Reinsbach[2], Arnaud Muller[1], Nathalie Nicot[1], Demetra Philippidou[2], Laurent Vallar[1] and Stephanie Kreis[2,*]

[1]Genomics Research Unit, Centre de Recherche Public de la Santé, L-1526 Luxembourg, Luxembourg and [2]Signal Transduction Laboratory, Life Sciences Research Unit, University of Luxembourg, L-1511 Luxembourg, Luxembourg

ABSTRACT

MicroRNAs (miRNAs) are ubiquitously expressed small non-coding RNAs that, in most cases, negatively regulate gene expression at the post-transcriptional level. miRNAs are involved in fine-tuning fundamental cellular processes such as proliferation, cell death and cell cycle control and are believed to confer robustness to biological responses. Here, we investigated simultaneously the transcriptional changes of miRNA and mRNA expression levels over time after activation of the Janus kinase/Signal transducer and activator of transcription (Jak/STAT) pathway by interferon-γ stimulation of melanoma cells. To examine global miRNA and mRNA expression patterns, time-series microarray data were analysed. We observed delayed responses of miRNAs (after 24–48 h) with respect to mRNAs (12–24 h) and identified biological functions involved at each step of the cellular response. Inference of the upstream regulators allowed for identification of transcriptional regulators involved in cellular reactions to interferon-γ stimulation. Linking expression profiles of transcriptional regulators and miRNAs with their annotated functions, we demonstrate the dynamic interplay of miRNAs and upstream regulators with biological functions. Finally, our data revealed network motifs in the form of feed-forward loops involving transcriptional regulators, mRNAs and miRNAs. Additional information obtained from integrating time-series mRNA and miRNA data may represent an important step towards understanding the regulatory principles of gene expression.

INTRODUCTION

MicroRNAs (miRNAs) have been discovered in 1993, and initially, these small non-coding RNAs have not attracted much interest from the scientific community (1). However, in recent years, it has emerged that the highly conserved and ubiquitously expressed miRNAs are of paramount importance for the regulation of gene expression in humans, animals and plants (2). Thus far, >1600 mature miRNAs have been identified in humans (mirBase version 19), and each miRNA is predicted to regulate several hundreds of target genes, leading to the conservative estimate of >60% of human protein-coding genes being regulated by miRNAs (3,4). The binding of miRNAs to their target mRNAs generally results in mRNA down-regulation or degradation, with subsequent repression of protein synthesis (2,5). A common and established feature is that miRNAs do not need an entirely complementary region in the 3′ UTR of the target gene mRNA to bind to but can do with varying numbers of mismatching nucleotides. This renders *in silico* predictions of miRNA target genes very difficult, and thus far no efficient algorithm exists, which is able to reliably predict all, but no false-positive, target genes (6).

Given the large number of protein-encoding genes that miRNAs can regulate post-transcriptionally, it is evident that they modulate and fine-tune almost all biological processes (7). Consequently, miRNAs have been implicated in the regulation of processes that promote cancer growth, or conversely, in processes that might prevent cancers and other diseases from developing (8–11). Considering their tremendous regulatory potential and their often tissue- and disease-specific expression patterns (12), de-regulated individual miRNAs or altered global miRNA expression profiles could be indicative of disease risks and burdens; therefore, miRNAs are currently

*To whom correspondence should be addressed. Tel: +352 46 66 44 6884; Fax: +352 46 66 44 6435; Email: stephanie.kreis@uni.lu

The authors wish it to be known that, in their opinion, the first two authors should be regarded as joint First Authors.

being assessed as possible biomarkers to aid diagnosis and prediction of different types and stages of cancers, including melanoma (13,14). In addition, miRNAs are discussed as targets for cancer therapeutics and as possible biomarkers (15). Despite recent progress in understanding miRNA effects on cell behaviour, the precise mechanisms and implications of miRNA actions are currently debated. To answer these questions, the dynamic regulation of miRNA expression changes will have to be considered, which thus far has been largely neglected (16).

The initial point of regulation of miRNA biogenesis, the transcription of miRNA genes, is a tightly controlled multi-step process, which often involves auto-regulatory feedback loops and feed-forward loops (FFLs) in which miRNAs participate together with transcription factors (TFs) (7,17–19). Gene expression, in general, results in variable levels of gene transcripts and proteins. Together with expression noise, the magnitude of which is influenced by intrinsic and extrinsic factors (20), gene transcription and its inferred regulatory networks can be considered as 'dynamic information processing systems' (21–23). However, the fluctuations in transcript levels (expression noise) have to be counter-balanced by a certain level of robustness in the biological responses, and this sturdiness is thought to be maintained by miRNAs (24). In this context, the integration of matching mRNA and miRNA data sets will become increasingly important. Recently, Muniategui *et al.* (25) have reviewed and grouped mathematical and computational approaches for analysing the interplay between miRNAs and mRNA into three main categories: dependency analysis, linear regression and Bayesian methods. It was further emphasized that models combining heterogeneous experimental data, such as time-series data, would be more reliable to predict miRNA–mRNA interactions. Dynamic data of a given biological system can add valuable information to a better understanding of the underlying cellular processes that might be missed using cross-sectional data that only focus on single time points (26). Recently, Kim *et al.* (27) have analysed complex network dynamics by using time-series–derived expression data; with principal network analysis, they were able to capture major activation patterns from two data sets and to generate the associated sub-networks and their interactions. Jayaswal *et al.* (28), in contrast, used odds ratio statistics to perform an integrative analysis on matched miRNA and mRNA time-course microarray data, which identified miRNAs with regulatory potential and their targeted mRNAs. Associations between TFs and miRNAs in monocytic differentiation were also determined in a time-lagged expression correlation analysis, which identified 12 TFs regulating the expression of several key miRNAs (29). The importance of time-series gene expression data was also underscored by a recent review in which Bar-Joseph *et al.* (30) expertly summarized current knowledge on this topic: different biological scenarios lead to different response patterns or programs, resulting in cyclic, sustained or most commonly peaked impulse responses after a stimulus and/or environmental perturbations.

To investigate whether integrative time-series–derived data would provide a means to better explain and identify complex regulatory interactions, we generated data sets representing a melanoma cell–derived miRNome and transcriptome (mRNAs) analysed at different time points after a transcriptional activation stimulus. We developed an analysis pipeline and combined known methods to extract information from these dynamic data sets, aiming at the visualization of functional variations that are connected to expression changes. We stimulated melanoma cells with interferon-γ (IFN-γ), a type II cytokine, which is known to induce STAT1-mediated growth inhibition and anti-proliferative effects in these cells (31,32). We set out to find potential explanations for these biological effects by integration of dynamic miRNA and mRNA data sets. Time-series differential expression analyses were performed, mainly in the form of contrasts between experimental conditions (IFN-γ–treated samples versus untreated controls) using the R/Bioconductor package 'limma' (33), in combination with profile correlation analysis, Ingenuity® Pathway Analysis (IPA) and data visualization with Circos (34). We and others have shown before that activation of STAT TFs specifically up-regulates the expression of several miRNAs in a time- and dose-dependent manner (35–40). In the current study, we have observed a delayed response of the miRNome with respect to the transcriptome, and have dynamically connected biological functions involved in cellular responses to IFN-γ. The up-regulation of several TFs downstream of STAT1, which might be required for full transcriptional activation of most miRNAs as well as different processing times of primary miRNA transcripts (41), might account for this delayed miRNome response. In addition, we have identified several FFLs including TFs, miRNAs and mRNAs. We argue that the integration of time-series–derived miRNA and mRNA expression data provides valuable information for generation of biological networks and is highly relevant for fully understanding the regulation of biological responses and processes.

MATERIALS AND METHODS

Time-series experiments

To investigate the dynamic regulation and potential co-regulation of miRNAs and mRNAs, time-course experiments were performed as described before (40). An overview of the experimental setup is shown in Supplementary Figure S1. Briefly, the time-course experiments were carried out using the human A375 melanoma cell line (ATCC, CRL-1619™). Cells were seeded into six-well plates at a density of 50 000 cells/well and were either left untreated (ctrl) or stimulated with human IFN-γ (PeproTech Inc., final concentration of 50 ng/mL) for the indicated time points. In parallel, a second control time-series experiment was performed including a pre-treatment step with 5 μM Janus kinase (Jak) inhibitor I (JII; Calbiochem), added 1 h before commencing IFN-γ stimulation. For microarray applications, RNA was extracted using the miRNeasy Mini kit (Qiagen); for

quantitative real-time PCR (qPCR) validations, TRIsure (Bioline) was used. The description of the qPCR method and primer sequences is given in Supplementary Data (Supplementary Table S1). We extracted and analysed RNAs from three biological replicates, each consisting of three technical replicates. RNA quality was assessed using Nanodrop 2000 Spectrophotometer (Thermo Scientific) and Agilent 2100 Bioanalyzer (Agilent Technologies).

miRNA and mRNA microarray expression profiling

miRNA microarrays were performed using the Affymetrix GeneChip® miRNA 2.0 Array technology as described by Reinsbach *et al.* (40). In addition, matching mRNA microarrays for selected time points (ctrl, 3, 12, 24, 48 and 72 h) were performed using Gene Chip® Human Gene 1.0 ST Array (Affymetrix, Santa Clara, CA, USA) on 17 samples. miRNA and mRNA microarray expression data are available at ArrayExpress (www.ebi.ac.uk/arrayexpress) under accession numbers E-MEXP-3544 and E-MEXP-3720, respectively.

Microarray data analysis

The workflow of data processing and analysis is outlined in Figure 1. Pre-processing of microarray data was performed with Partek® Genomics Suite version 6.5 (Partek®

Figure 1. Graphical representation of the computational workflow. In the first step, miRNA and mRNA array data were pre-processed and the quality was assessed using Partek® GS. A filtering step was included to select only expressed and detectable features. Co-expression analysis and identification of potential targets were performed directly on the paired miRNA-mRNA data. Differential expression analysis was performed using the 'limma' package of R/Bioconductor to identify significant differentially expressed mRNAs and miRNAs over time. Functional and pathway analysis together with identification of upstream regulators was carried out in IPA based on SDE molecules. The dynamic behaviour of gene regulation circuitry in response to IFN-γ stimulus was visualized as Circos plots.

GS) using the robust multi-chip analysis algorithm, which performs background adjustment, quantile normalization and probe summarization as described before (42). For mRNA data, GC content correction was used, as suggested by the default pipeline of Partek® GS. To decrease the number of uninformative features, we used a filtering step: features, for which the maximum expression over all arrays did not reach a signal intensity of 7 in a $\log_2$ scale, were removed. Different methods ['betr' (43), 'timecourse' (44) and 'limma' (33)] to identify significantly differentially expressed (SDE) miRNAs and mRNAs were tested (Supplementary Data and Supplementary Table S2). In this study, linear models and the empirical Bayes method from the 'limma' package of R/Bioconductor were used for differential analysis of the miRNA and mRNA time-series data sets as described before (45). In addition, to obtain a list of features significantly regulated at each time point, we used the same 'limma' model and a set of contrasts, comparing expression in IFN-γ–treated samples versus untreated controls. To control for false discovery rates (FDR), we used the Benjamini–Hochberg method to adjust *P*-values.

Microarray data were visualized as heat maps using a standard eponymous function of R. A hierarchical clustering algorithm was applied to determine similar patterns in miRNA and mRNA expression profiles. Clustering was supported by bootstrapping using the 'clusterCons' package of R (46).
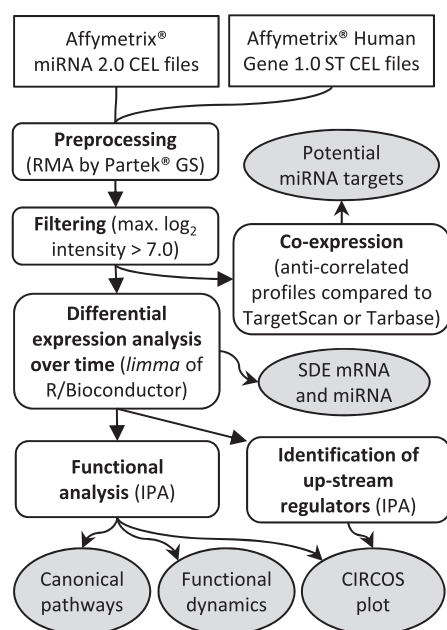
Correlation analyses using CoExpress

Negatively correlated miRNA-mRNA pairs were determined by the in-house developed stand-alone software tool CoExpress (freely available at www.bioinformatics.lu/CoExpress), which performs interactive detection of correlated profiles in large expression data sets. The software allows single-data type analysis for identification of miRNA-mRNA co-expression events as well as two-data type analysis for detection of correlated miRNA-mRNA expressions. Details on CoExpress are given in the Supplementary Data section.

Data mining and visualization

Canonical pathway analysis. Lists of mRNAs and miRNAs, differentially expressed between each condition (time points) and untreated controls (with FDR < 0.001), were uploaded in the IPA tool (Ingenuity® Systems, www.ingenuity.com) and analysed based on the IPA library of canonical pathways (content date 2012-05-08). The significance of the association between each list and a canonical pathway was measured by Fisher's exact test. As a result, a *P*-value was obtained, determining the probability that the association between the genes in our data set and a canonical pathway can be explained by chance alone.

Functional analysis. To identify biological functions and/or diseases that were most significant to our data sets functional analysis was done. As in canonical pathway analysis, features that met the FDR cut-off of 0.001 when comparing each condition with the untreated control were analysed by IPA. Right-tailed Fisher's exact test was used to calculate a significant *P*-value for

each functional category as referenced in Ingenuity® Knowledge Base. The obtained *P*-value was further adjusted using the Benjamini–Hochberg correction. We focused our analysis on IPA categories with an adjusted $P \leq 0.01$ (presented in at least one time point) directly related to cellular functions and diseases, providing dynamical information about enriched biological functions. *Upstream regulator analysis*. Based on previous knowledge of expected effects between transcriptional regulators (TRs) and their target genes stored in the Ingenuity® Knowledge Base upstream regulator analysis was performed. Two statistical measures, standard in IPA, were used to detect potential TRs: an overlap *P*-value and an activation *Z*-score. First, the analysis examined how many known targets of each TR were present in our data set, resulting in an estimation of an overlap *P*-value. We set a threshold of an overlap $P < 0.05$ to identify significant upstream regulators. Second, the known effect (activation or suppression) of a TR on each target gene was compared with observed changes in gene expression. Based on concordance between them, an activation *Z*-score was assigned, showing whether a potential TR was in 'activated' (*Z*-score > 2), 'inhibited' (*Z*-score < -2) or uncertain state.

Circos plots. We built Circos plots (34) to simultaneously visualize activated/inhibited upstream TRs (mainly consisting of TFs, Histone deacetylases (HDACs) and nuclear receptors), miRNAs and selected biological functions for each time point. Briefly, we first included known activated/inhibited upstream TRs based on SDE genes for each time point ('inferred TFs'). Next, we selected miRNAs targeting these inferred TFs from TarBase v.6 (http://www.microrna.gr/tarbase) (47). Then, we identified other non-TR target genes of these miRNAs and created a network representing inferred TRs, miRNAs targeting these TRs and mRNAs, targeted either by TRs and/or by selected miRNAs. Importantly, only mRNAs and miRNAs, which showed significant differential expression in at least one condition (compared with untreated controls), were included in the network. Next, the identified SDE mRNAs (that are targeted by TR and/or miRNA) were subjected to IPA for functional annotation. To increase readability of the final Circos plots, we combined biologically related Ingenuity® functions into 12 functional categories. Finally, we visualized identified networks and connections between molecules and functional categories using Circos.

Identification of regulatory loops. To identify regulatory loops involving TRs, miRNAs and their common targets, we first targeted our approach to build networks of previously inferred TRs and their corresponding SDE mRNA targets for each time point. Secondly, SDE miRNAs were overlaid onto the networks. Next, connections were associated with miRNAs that share the same targets as TRs and which were at the same time targeted by the TRs (a specific type of FFL in the form of 'TF → miRNA–targets', edges from both regulators to target). Finally, a subset of FFLs from the networks was extracted based on biological significance. All the connections of these FFLs were based on experimentally validated interactions referenced in the Ingenuity® Knowledge Base, and

the mRNAs and miRNAs were selected based on their connectivity and their significance of differential expression at each time point.

RESULTS

In the current study, we analysed and integrated matched time-series miRNA and mRNA microarray data, which were generated from melanoma cells after IFN-γ stimulation as outlined in Supplementary Figure S1. The previously described dynamic miRNA data sets (40) were combined with newly generated and matched mRNA expression levels from the same samples for selected time points. Optimal sampling time points had been determined before by monitoring expression changes in response to IFN-γ stimulation of a small number of miRNAs and genes [data not shown and (40)]. Given a fixed budget, we mostly opted for microarray duplicates rather than triplicates and could therefore include more time points. However, to increase sensitivity and to control for batch effects, we performed an additional third replicate for 24, 48 and 72 h. Two replicates of paired miRNA–mRNA microarray expression data were obtained for the control; for 3, 12, 24, 48 and 72 h of IFN-γ–treated samples; and for the JII-pre-treated control (JII ctrl). We have shown before that JII prevented the phosphorylation and thus activation of STAT1 TF and its downstream actions, and therefore served as an additional control (40).

Analysis pipeline for identification of differentially expressed mRNAs and miRNAs

The outline of computational analysis steps as applied to all data sets is depicted in Figure 1. A multi-step approach was performed to identify SDE miRNAs and mRNAs over time. First, we checked the quality of the time-series mRNA data sets using Partek® Genomics Suite. No outlier microarrays or batch effects were detected (data not shown). If not stated otherwise, we included the third mRNA replicates in the analysis. As illustrated by the correlation study (Supplementary Figure S2), reproducibility for mRNA expression data was evaluated by calculating coefficients of determination (r^2) as previously done for miRNA expression data (40). Average coefficient of determination with 95% confidence was equal to 0.979 ± 0.005 for both replicates and 0.903 ± 0.004 for non-replicates, showing the robustness of expression data sets. After pre-processing and quality control, a filtering step was included (as outlined in 'Materials and Methods' section), which reduced the number of considered features for both data sets, and improved the estimated FDR. In total, 16 193 mRNAs (out of 33 279) and 160 miRNAs (out of 1100) passed the filtering and were considered for further analysis. To identify the best possible method for analysing these data sets, we first compared three methods available as R/Bioconductor packages: 'limma', 'betr' and 'timecourse'. Empirical Bayes methods and linear modelling ('limma') performed better than other methods in terms of flexibility (as there is no need to have equal numbers of experimental replicates) and in terms of FDR on permutated and simulated data
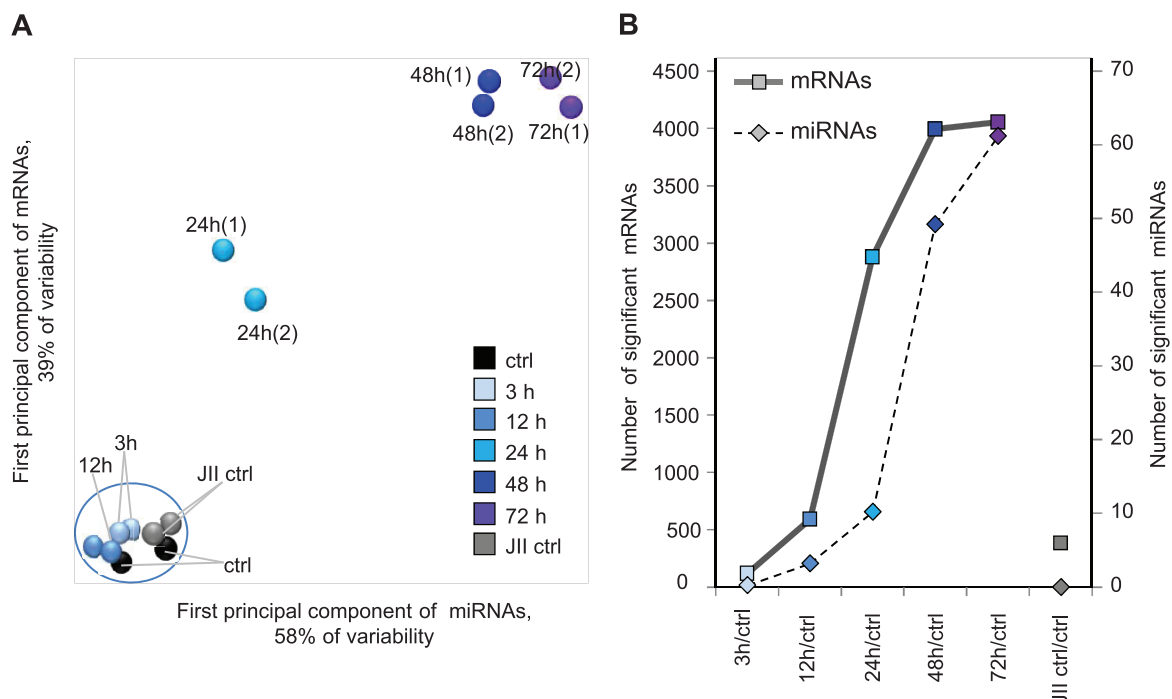
(Supplementary Data). Therefore, differential expression analysis was performed using the limma package. For further analyses, a threshold FDR < 0.001 was applied, resulting in 65 miRNAs and 6056 mRNAs SDE over all time points. Using the same model and contrasts between expression levels in IFN-γ–treated samples versus untreated controls, we identified SDE mRNAs for each time point separately.

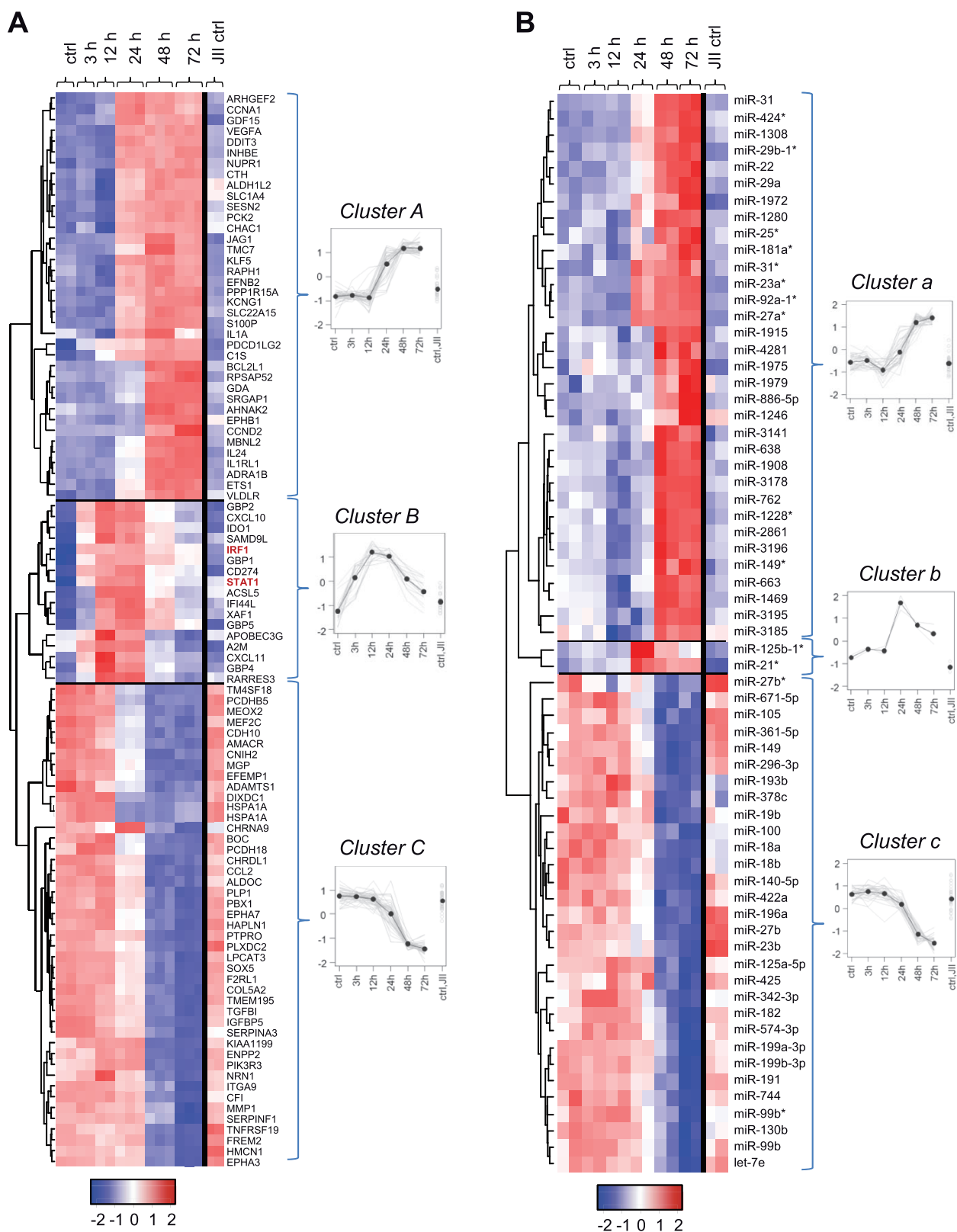## Dynamic expression changes of miRNAs are delayed relative to mRNA expression changes

To obtain a global view of the behaviour of filtered and paired miRNA–mRNA expression data, principal component analysis (PCA) was performed on each of the two data sets. The first principal component of two independent PCAs was plotted (Figure 2A), showing transcriptome evolution over time, with the horizontal axis representing variability in miRNome and the vertical axis representing variability in mRNAs. Remarkably, the principal components of both mRNA and miRNA data showed strong and reproducible time effects and accounted for 39% of data variability for mRNA and 58% for miRNA. Owing to the properties of the principal component, this representation shows the main variability of mRNA and miRNA expression levels of all samples. Early time points (3 and 12 h) and both controls (untreated and JII pre-treated) cluster together implying that the overall changes of the transcriptome were comparable with the average variability between replicates. The behaviour

suggests that miRNA expression changes after IFN-γ stimulation were delayed with respect to mRNA expression changes, which were observed already at earlier time points. Interestingly, miRNA levels continued to change until 72 h, whereas mRNA levels were not altered significantly after 48 h. This suggests that mRNA expression levels adapt faster to the cytokine stimulus, possibly to initiate a rapid inflammatory response, which is then followed by a second transcriptional wave where miRNAs are involved in the regulatory cascade to fine-tune and adjust the system responses in the form of feedback regulators. Such miRNA-mediated feedback and FFLs have been described as common network motifs (48), and this observation was further supported by our 'limma' differential expression analysis. Several contrasts (two-class comparisons) were generated through comparisons between IFN-γ–treaded samples and untreated controls. The resulting number of significant mRNAs and miRNAs (FDR < 0.001) is shown in Figure 2B, where biggest effects of cytokine stimulation on the transcriptome were scored between 12 and 24 h for mRNAs and between 48 and 72 h for miRNAs. At 24 h, ~45% of all significantly expressed mRNAs were up-regulated, whereas expression changes of miRNAs (>50%) occurred later (at 48 h).

Hierarchical clustering based on the expression profiles of significantly regulated mRNAs and miRNAs is shown in Figure 3. For better readability, we only show the top 100 SDE mRNAs and all 65 SDE miRNAs. Further analyses were performed using all significantly

Figure 2. Projection of dynamic changes of the transcriptome and the miRNome of melanoma cells after IFN-γ stimulation. (**A**) PCA visualizes the evolution of both data sets over time, with the vertical axis corresponding to the first principal component of mRNA data and the horizontal axis showing the principal component of miRNA data. The percentage of variability in the data sets represented by each axis is shown. The dots represent sample duplicates (complete arrays) for the indicated stimulation times. (**B**) The number of SDE mRNAs and miRNAs with FDR < 0.001 for each condition compared with the untreated control is shown. The maximum gradient was observed between 12 h/ctrl and 24 h/ctrl for mRNAs and between 24 h/ctrl and 48 h/ctrl for miRNAs.

Figure 3. Heat maps representing the time evolution of the top 100 mRNAs and all 65 differentially regulated miRNAs detected through multi-class 'limma' analysis (FDR < 0.001). Standardized expression values for each feature were reordered by hierarchical clustering, resulting in three pronounced clusters depicted on the right of each heat map. Each cluster contains member gene or miRNA profiles (grey lines) and mean expression values (dots). (**A**) The top 100 significantly expressed and annotated mRNAs fall into three main groups (cluster A, B, C). Names of TFs involved in IFN-γ signalling are marked in red. Clustering was supported by bootstrapping using the 'clusterCons' package of R. Altered cluster annotations were only observed for two genes (A2M and APOBEC3G), which after bootstrapping were more likely to belong to cluster C rather than B. (**B**) The majority of all SDE miRNAs belong to two clusters (a and c), with delayed up- or down-regulation after 24 h, respectively. Cluster b contains only two miRNAs (miR-125b* and miR-21*).

regulated mRNAs (FDR < 0.001) (Supplementary Figure S3). Based on this approach, we have identified three main clusters for mRNAs (Figure 3A), supported by a boot-strapping analysis using 'clusterCons' package of R (1000 iterations of hierarchical clustering with Euclidian distance). Cluster A showed delayed mRNA up-regulated expression reaching a plateau at 48 h, whereas cluster B contained genes responding rapidly to IFN-γ stimulation. The average profile showed up-regulation after IFN-γ stimulation, followed by a decrease in expression down to almost baseline levels after 72 h. This latter cluster included well-known TFs involved in IFN-γ–stimulated signalling: STAT1 and IRF1 and also chemokines (CXCL10 and CXCL11), which are typically up-regulated by IFN-γ treatment (49). Finally, cluster C included down-regulated mRNAs (after 24 h) that remained at low expression levels until 72 h. Figure 3B depicts miRNA expression changes for the selected time points. We have previously observed that miRNA expression patterns significantly change only after 48 h (40), and were able to further confirm these alterations using the herein described different analysis pipeline. The JII control samples (72 h) demonstrate that mRNA and miRNA regulations were diminished by blocking the Jak/STAT signalling cascade, indicating that the observed expression changes were caused by IFN-γ–activated downstream regulators. It is known that IFN-γ treatment activates a variety of target genes and among those several TFs (49). Our data again suggest that these activated TFs then start a second wave of transcriptional activations, which seems to include many miRNAs the expression levels of which subsequently increase with a certain time delay.

Correlation and validation of dynamically regulated mRNAs and miRNAs

Next, we identified positively and negatively correlated miRNA–mRNA pairs using CoExpress, an in-house bio-informatics tool (http://www.bioinformatics.lu/ CoExpress), which combines correlation analysis with miRNA target gene predictions (see Supplementary Data and Supplementary Table S3). A negative dynamic correl-ation between a given miRNA and a predicted target mRNA could be the first indicator of a potential direct interaction. Supplementary Figure S4A summarizes the number of co-expressed mRNAs for each of the co-expressed miRNAs ($|r| > 0.95$). The first nine miRNAs with most negatively correlated events (miR-31, -1308, -424*, -29b-1*, -23a*, -92a-1*, -29a, -22, -27a*) belonging to cluster a (Figure 3B) show a clear tendency to have more negatively correlated expressions with mRNAs, whereas miR-27b (cluster c) had the highest proportion of positively correlated events. Interestingly, increasing the stringency of the correlation threshold resulted in a higher proportion of negatively correlated events (Supplementary Figure S4B). Microarray-measured expression levels were validated by qPCR for nine miRNA–mRNA pairs that were selected based on correlation, confirming expression patterns for all tested pairs (Supplementary Figure S5). We mainly focussed on two miRNAs, miR-29b-1* and miR-424*, that we have previously shown to be among the top

10 dynamically up-regulated miRNAs after IFN-γ treatment (40).

CoExpress was used to identify negatively correlated and biologically interesting mRNAs that are known to be involved in tumourigenesis of melanoma or other ma-lignant tumours (50–53). TIAM1 (T-cell lymphoma invasion and metastasis 1) and IGFBP5 (insulin-like growth factor–binding protein 5) were dynamically anti-correlated with miR-29b-1*. MMP1 (matrix metallo-peptidase 1) and SOX5 [SRY (sex-determining region Y)-box 5] showed inverse correlations over time with miR-424*, while VCAN (versican) was negatively correlated with both miRNAs. Expression levels of all JII-pre-treated samples remained largely unchanged over time for SOX5 and HDAC9, indicating that the observed changes in the miRNA levels were likely caused by the IFN-γ–induced Jak/STAT signalling. In contrast, for MMP1 and IGFBP5, mRNA levels in the JII-treated control samples were also down-regulated, suggesting additional IFN-γ–independent effects. Taken together, quality measures as well as validation of microarray results confirmed high quality and reproducibility of both data sets. In the following steps, we combined and analysed these time-series–derived data sets representing dynamic expression changes of the melanoma miRNome and transcriptome to identify interactions that only become visible over time.

Functional annotation of dynamically regulated mRNAs and miRNAs

To better understand which and how biological functions are affected by differentially regulated mRNAs and miRNAs over time, we performed functional annotations in Ingenuity® Systems (IPA) based on SDE mRNAs and miRNAs (each condition was compared with untreated controls). All 62 significant functional categories reported by IPA (adjusted $P < 0.01$) are presented in Figure 4. To show the time evolution among the categories, the smallest adjusted P-values of member func-tions were taken for each category and each time point. Colouring was performed based on scaled $\log_{10}$-trans-formed adjusted P-values, with white colour correspond-ing to adjusted $P \geq 0.01$ and dark grey corresponding to the smallest adjusted P-value for a given category among all time points. Visualization of the resulting dynamics allowed for comparison of functional enrichment between the five time points. We found five groups with temporal differences in enriched functional responses to IFN-γ treatment. The first group included very early cellular reactions to IFN-γ, with enrichment of functions mainly observed between 3 and 12 h. In the second and largest group, functional enrichments peaked around 12 h after treatment and included several categories of immune and inflammatory responses. A third group showed smallest P-values for functions at intermediate time points 24 h after IFN-γ treatment, while only four categories, including 'cancer' and 'post-translational modifications', had enrichment peaks at 48 h. We have previously observed that most miRNAs are being differ-entially expressed at this time point (40), suggesting a

3h/ctrl	12h/ctrl	24h/ctrl	48h/ctrl	72h/ctrl	Jll ctrl/ctrl	
4.3e-04	1.2e-03	3.1e-03	n/s	1.9e-03	2.2e-02	Hematological Disease
6.1e-04	3.1e-03	2.5e-03	n/s	1.5e-03	4.3e-02	Hematopoiesis
3.8e-05	3.8e-04	1.0e-02	n/s	n/s	n/s	Organismal Survival
1.3e-03	6.5e-03	1.8e-02	n/s	3.5e-02	3.2e-02	Respiratory Disease
3.8e-03	1.9e-02	n/s	n/s	n/s	4.3e-02	Lymphoid Tissue Structure and Development
7.7e-04	6.5e-03	3.1e-02	n/s	3.5e-02	3.2e-02	Connective Tissue Development and Function
1.3e-03	6.5e-03	3.1e-02	3.9e-02	2.3e-02	4.3e-02	Organ Development
7.7e-04	5.6e-03	3.1e-02	8.4e-03	1.5e-03	1.5e-02	Skeletal and Muscular System Development and Function
5.2e-04	5.4e-04	1.2e-02	n/s	4.1e-03	2.6e-02	Gene Expression
1.6e-03	1.5e-03	4.0e-03	n/s	n/s	4.3e-02	Cell Signaling
2.6e-02	1.3e-13	2.3e-04	1.5e-02	1.3e-03	5.1e-03	Endocrine System Disorders
n/s	1.3e-13	2.7e-04	1.2e-02	1.7e-03	5.1e-03	Metabolic Disease
1.8e-02	2.3e-06	2.1e-04	4.8e-05	1.6e-05	4.8e-03	Neurological Disease
9.2e-06	7.4e-13	8.8e-05	2.1e-02	1.2e-03	4.3e-02	Infectious Disease
1.8e-02	1.2e-04	3.1e-02	n/s	n/s	4.3e-02	Tissue Morphology
1.8e-02	5.6e-04	2.0e-02	n/s	2.3e-02	n/s	Tumor Morphology
9.5e-05	5.2e-10	1.4e-07	2.1e-02	1.3e-02	5.1e-03	Connective Tissue Disorders
2.0e-06	3.9e-14	3.3e-11	7.9e-03	1.5e-02	3.7e-03	Dermatological Diseases and Conditions
9.5e-05	3.2e-10	1.4e-07	7.1e-04	1.3e-02	5.1e-03	Inflammatory Disease
9.5e-05	5.2e-10	1.4e-07	4.8e-05	9.8e-04	5.1e-03	Skeletal and Muscular Disorders
8.7e-06	1.5e-18	3.4e-06	8.3e-03	2.1e-02	5.0e-03	Immunological Disease
1.8e-03	4.8e-09	3.2e-05	n/s	n/s	2.6e-02	Ophthalmic Disease
4.3e-04	1.3e-05	6.1e-04	n/s	1.5e-03	1.6e-02	Hematological System Development and Function
6.1e-04	1.3e-05	6.1e-04	n/s	n/s	1.6e-02	Immune Cell Trafficking
3.8e-05	1.4e-06	6.4e-06	2.6e-04	1.1e-04	9.1e-03	Cell Death and Survival
1.9e-03	1.7e-04	5.4e-04	n/s	n/s	2.4e-02	Inflammatory Response
4.5e-03	1.5e-03	8.7e-03	1.6e-02	2.0e-02	1.8e-02	Molecular Transport
6.1e-04	1.3e-05	1.6e-02	n/s	n/s	4.3e-02	Cell-mediated Immune Response
1.8e-02	3.1e-03	n/s	n/s	3.7e-02	4.3e-02	Cellular Compromise
8.5e-03	2.0e-04	n/s	n/s	n/s	n/s	Antimicrobial Response
1.0e-02	6.5e-03	3.1e-02	4.7e-02	n/s	2.6e-02	Hair and Skin Development and Function
4.5e-03	1.5e-03	2.3e-02	n/s	n/s	n/s	Vitamin and Mineral Metabolism
1.8e-02	1.3e-02	1.3e-05	7.1e-04	3.5e-02	3.9e-02	Hepatic System Disease
1.8e-02	1.3e-03	1.3e-05	7.1e-04	2.1e-02	4.3e-02	Organismal Injury and Abnormalities
1.8e-02	4.0e-04	5.6e-07	3.5e-05	1.4e-04	4.3e-02	Cellular Assembly and Organization
1.8e-02	4.0e-04	5.6e-07	3.5e-05	1.4e-04	4.3e-02	Cellular Function and Maintenance
2.7e-03	1.5e-02	5.6e-07	3.5e-05	2.4e-04	4.3e-02	Nervous System Development and Function
7.7e-04	6.3e-05	5.6e-07	3.5e-05	2.4e-04	1.5e-02	Tissue Development
1.5e-03	1.6e-05	5.6e-07	3.5e-05	2.4e-04	1.8e-02	Cell-To-Cell Signaling and Interaction
1.3e-03	1.2e-03	1.3e-06	3.1e-04	2.4e-05	1.5e-02	Organismal Development
6.8e-03	6.5e-03	3.0e-04	4.7e-02	n/s	1.8e-02	Renal and Urological System Development and Function
1.8e-02	4.4e-02	8.7e-03	1.6e-02	2.0e-02	1.8e-02	Amino Acid Metabolism
n/s	n/s	4.0e-03	n/s	n/s	n/s	Nutritional Disease
1.8e-02	4.4e-02	3.7e-03	2.1e-02	n/s	3.5e-02	Reproductive System Development and Function
4.3e-04	3.0e-04	2.3e-05	7.6e-04	6.8e-04	1.5e-02	Cellular Growth and Proliferation
4.3e-04	3.0e-04	1.8e-04	2.5e-03	8.2e-04	8.0e-03	Cellular Development
6.1e-04	3.1e-03	3.0e-04	4.6e-03	2.3e-03	2.6e-02	Cell Morphology
1.3e-03	4.3e-03	1.2e-03	3.9e-02	2.3e-02	2.6e-02	Embryonic Development
n/s	2.2e-02	1.3e-02	5.2e-03	1.1e-02	n/s	Post-Translational Modification
n/s	9.7e-03	1.3e-02	5.2e-03	1.1e-02	n/s	Protein Synthesis
4.3e-04	3.7e-05	8.1e-13	1.3e-14	2.9e-14	3.7e-03	Cancer
1.8e-02	1.3e-03	1.5e-02	1.2e-04	2.7e-03	1.5e-02	Hereditary Disorder
4.8e-04	1.3e-05	7.2e-06	1.1e-07	9.3e-08	3.7e-03	Cellular Movement
1.8e-03	1.3e-13	2.0e-08	1.1e-11	3.1e-14	5.1e-03	Gastrointestinal Disease
6.7e-03	1.4e-03	1.1e-05	4.4e-06	1.6e-08	2.6e-02	Reproductive System Disease
n/s	4.4e-02	1.2e-02	3.8e-03	1.6e-04	4.3e-02	Psychological Disorders
1.8e-02	2.4e-02	2.2e-03	2.4e-02	2.0e-03	n/s	Lipid Metabolism
1.8e-02	1.5e-02	2.2e-03	1.6e-02	2.0e-03	1.8e-02	Small Molecule Biochemistry
1.8e-02	1.9e-02	1.0e-03	5.3e-03	6.7e-04	1.5e-02	Cardiovascular Disease
6.8e-04	7.1e-04	6.2e-07	4.1e-05	1.4e-07	1.5e-02	Cardiovascular System Development and Function
2.6e-02	1.0e-02	3.7e-03	8.1e-03	1.7e-03	4.3e-02	Cell Cycle
n/s	n/s	4.0e-02	n/s	2.0e-02	6.4e-03	Renal and Urological Disease

Figure 4. Dynamic changes in inferred functional categories based on SDE mRNAs and miRNAs. The minimum adjusted *P*-values for member functions were combined to illustrate dynamic changes in all enriched functional categories obtained from IPA analysis ('n/s;: *P* > 0.05). The intensity of grey boxes represents scaled adjusted *P*-values (log-transformed) for each category: white—non-significant (>0.01), dark grey—smallest adjusted *P*-value for each category among the time points.
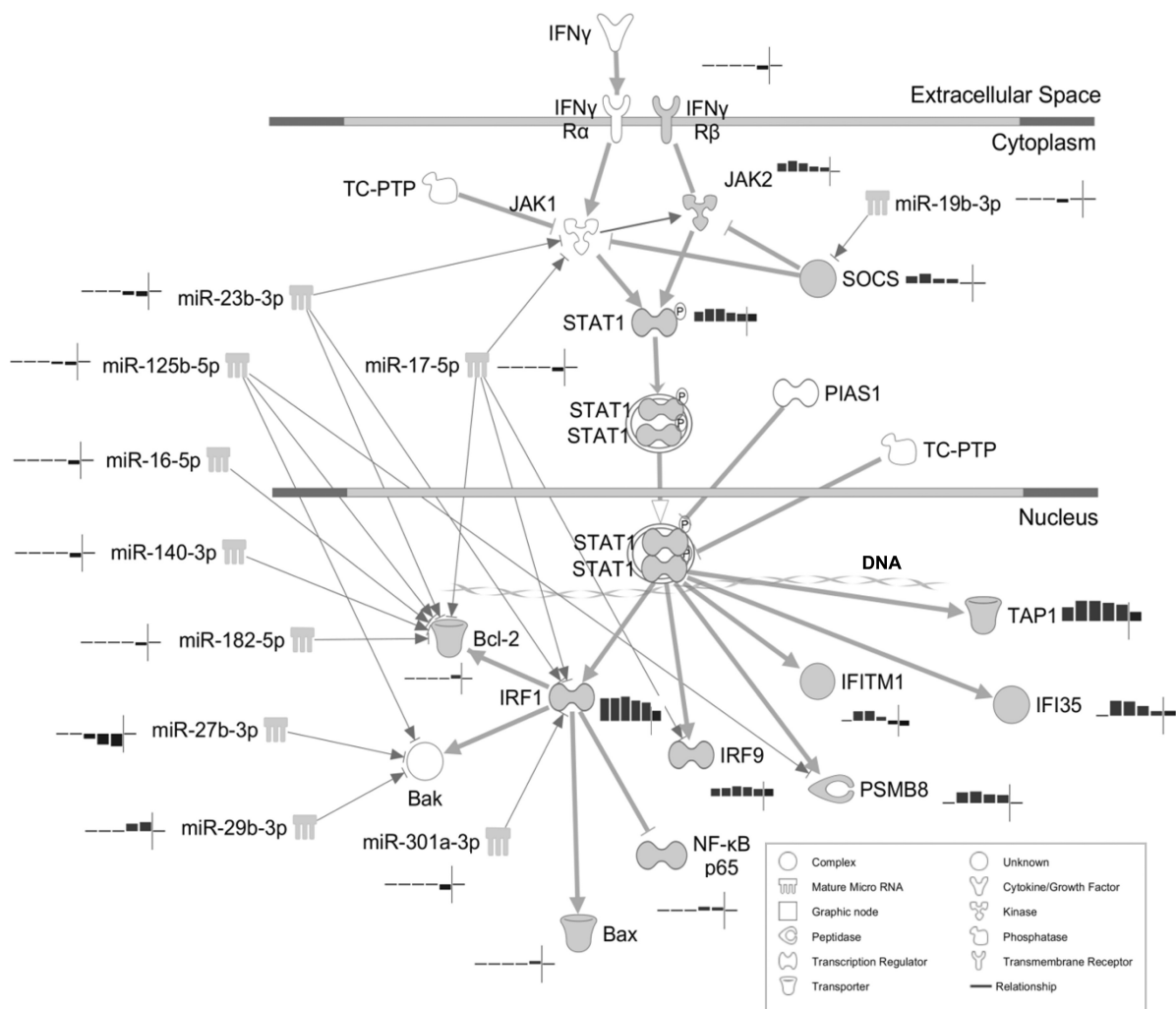
second wave of transcriptional changes, including the up-regulation of miRNAs after IFN-γ treatment. Finally, several categories such as 'cellular movement' and 'cell cycle' were only enriched very late after cytokine stimulation. Taken together, functional annotations of dynamic miRNA and mRNA expression changes after IFN-γ treatment showed that some categories were predominantly enriched at only one specific time point, emphasizing once more the importance of analysing time-series–derived data.

Dynamic features of the interferon pathway

To dissect the temporal behaviour of key players involved in interferon signalling in more detail, we analysed our data using the Ingenuity® Systems (IPA) program. As expected after stimulation with IFN-γ, the interferon signalling pathway was found to be highly significant,

especially at early time points (P-values for 3 h/ctrl and 12 h/ctrl were 4.8×10^{-13} and 2.0×10^{-13}, respectively). Figure 5 illustrates the IFN-γ sub-network as provided by the IPA Knowledge Base to which we connected expressed miRNAs that have been described to target the pathway-associated mRNAs (TarBase v.5 and TargetScan with total context score < −0.4) and were SDE in at least one time point. Most of the genes (65%) involved in the Jak/STAT signalling pathway were differentially expressed in at least one time point, which is depicted by small adjacent bar charts showing the experimentally measured expression levels over five time points (expression levels of the JII-treated control samples are shown on the far right side).

Although STAT1 needs to be phosphorylated to become activated, the gene itself is known to be up-regulated by IFN-γ stimulation (54), which was also confirmed here.

Figure 5. Representation of the top canonical pathway 'interferon signalling' detected when simultaneously analysing the mRNA and miRNA data sets with IPA. Parts related to IFN-α/β were removed, and SDE miRNAs targeting the detected genes of the pathway were added. Connections between miRNAs and their targets were established by IPA. Genes that were differentially expressed in at least one condition are marked with filled grey symbols. Expression changes at 3, 12, 24, 48 and 72 h with respect to untreated controls are shown as bar charts close to each molecule. For non-significant conditions, a line is shown instead of a bar. The last bar on the far right always corresponds to JII-treated control (72 h). Connections between main players of the signalling pathway are depicted as lines: relationships between miRNAs and target mRNAs are shown as thin lines, whereas relationships between TFs and target mRNAs are presented by thicker lines either indicating activation or repression.
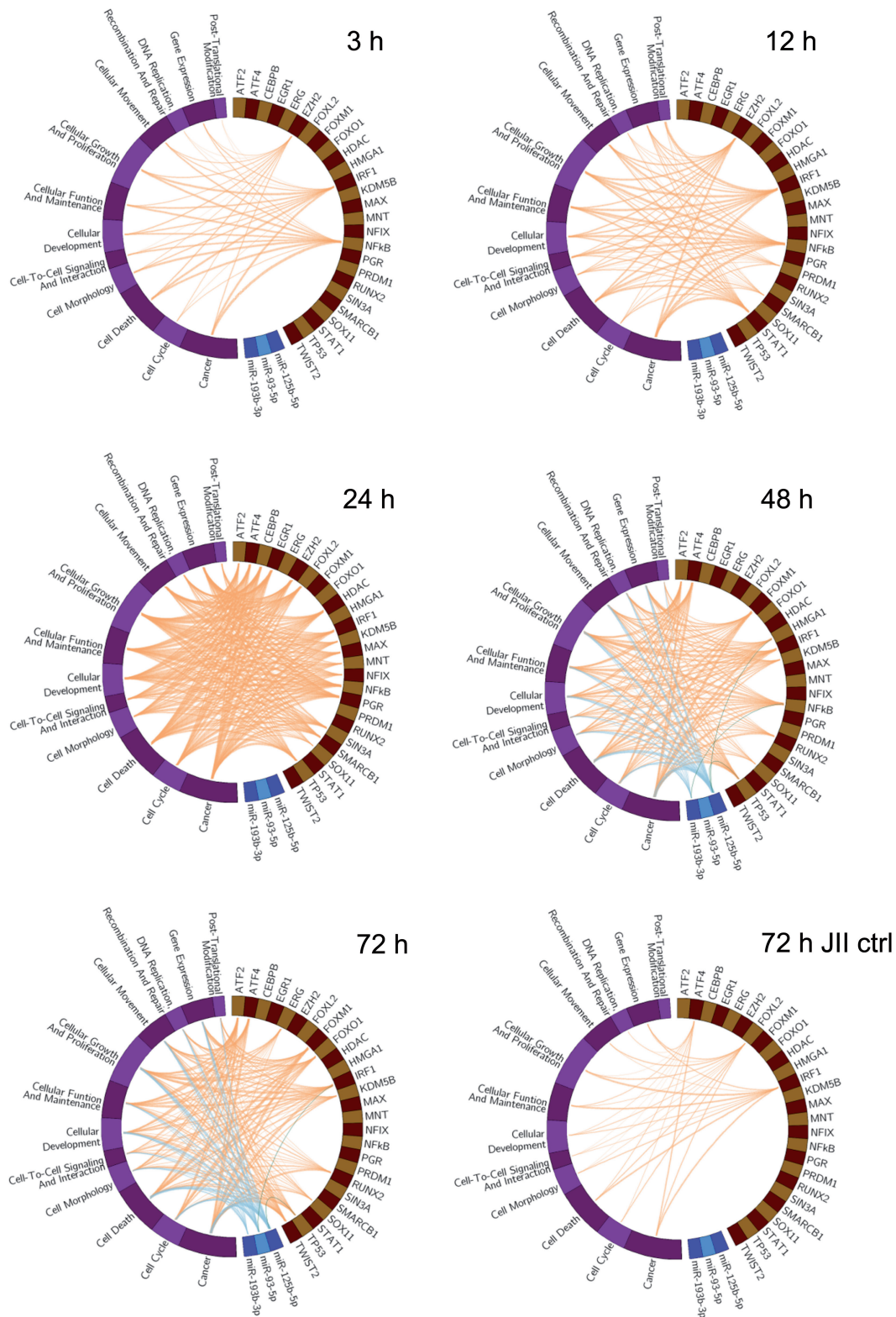
Three downstream targets of STAT1 (ARF1: ADP ribosylation factor 1, IRF9: interferon regulatory factor 9 and TAP1: antigen peptide transporter 1) show an immediate up-regulation after 3 h of interferon treatment, whereas most targets reached peak expression levels at 24 h (IRF1: interferon regulatory factor 1, IRF9, TAP1, IFITM1: interferon-inducible transmembrane protein 1, IFI35: interferon-induced 35-kD protein and PSMB8: proteasome β subtype 8). Consequently, the transcriptional targets of IRF1 (BCL-2 and BAX) became up-regulated in a second cascade, showing increased expression levels only at later time points. In line with previous observations [reviewed in (49)], at 12 h, we observed a moderate up-regulation of the suppressor of cytokine signalling (SOCS1), a negative feedback regulator, which reduces the activation of the Jak/STAT pathway. The temporal expression profiles of miRNAs connected to this pathway reveal inverse correlations with expression levels of their possible target genes. For example, miR-301a-3p was down-regulated at late time points, with its target gene IRF1 showing increased levels; miRNAs known to target BCL-2 were all down-regulated over time, whereas BCL-2 was up-regulated at 72 h. BAK, a target gene of IRF1 TF was not differentially regulated over time (white symbol) and miRNAs targeting this mRNA were either up-regulated (miR-29b-3p) or down-regulated (miR-27b-3p and miR-125b-5p). Interestingly, several mRNAs in the network showed similar expression profiles at 72 h in the IFN-γ–treated cells and in the JII-pre-treated cells (STAT1, IRF9, IFI35 and IFITM1), suggesting that feedback inhibitory processes were progressively developed in IFN-γ–treated cells recapitulating the phenotype observed in cells inhibited with JII. To summarize, visualizing dynamic expression data provides additional information about the interplay between miRNAs and mRNAs within the well-known IFN-γ signalling cascade.

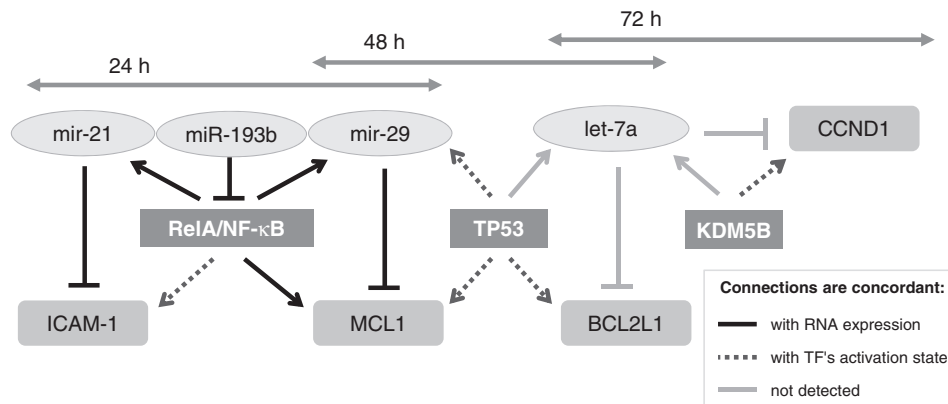### Integration of mRNA, upstream regulators and miRNA data

Although initially designed and used for displaying comparative genomic data (34), Circos plots have also been adapted to analyse mutations in cancer (55,56), metagenomic data (57) and dynamics of TF regulatory networks (58). Here, we have applied Circos plots to integrate data sets from three different sources, and to our knowledge, this is the first time that data from miRNome and transcriptome were simultaneously combined with annotated functions (Figure 6). We chose to work with biological functions because it provides more robust results than working with individual genes. To decrease complexity of the graphs and to allow for better readability, we only show those TRs, miRNAs and inferred functions that were selected through the pipeline described in 'Materials and Methods' section. Based on this integrative approach, we observed that miRNAs only become connected to TRs and biological functions at very late time points (48 and 72 h), indicating that they are activated by TRs downstream of the activated Jak/STAT signalling cascade. Similar to what was seen in Figure 5, Circos plots representing 3 h of

IFN-γ treatment and 72 h of JII-control treatments could almost be superimposed, suggesting that new connections scored at later time points were indeed brought about by Jak/STAT signalling. Although STAT1 was activated (by phosphorylation) after 15 min of IFN-γ treatment (40), it only became connected to annotated functions at the 12-h time point, while no direct interactions between STAT1 and selected miRNAs were detected at any time point. Furthermore, after 12 h of IFN-γ signalling, other TRs such as IRF1, nuclear factor of kappa light polypeptide gene enhancer in B-cells (NFκB) and Enhancer of zeste homolog 2 (Drosophila) (EZH2) were predicted to be active based on expression changes of their regulated genes. IRF1, a TF activated by STAT1, was actively 'communicating' throughout the experiment and could be involved in the downstream and delayed activation of several depicted miRNAs. At 48 and 72 h, we detected six connections between miRNAs and TRs. Additionally, the overall number of interactions between all players and inferred functions dramatically increased at these late time points. Again, this was not seen in the JII-treated negative control samples, implying that the established connections cannot be attributed to noise or mere 'ageing' of cells in culture. Of note, miR-93-5p, one of three miRNAs depicted in the Circos plots, was not present in the heat map (Figure 3B), as the hierarchical clustering was generated based on multi-class 'limma' analysis and the adjusted *P*-value for miR-93-5p was just above the selected threshold (with FDR = 0.0013). To generate Circos plots, we used contrasts between the 72-h time point and untreated samples in which miR-93-5p was detected as SDE, with an adjusted *P*-value of 0.0004 by two-class 'limma' analysis.

Common transcriptional regulatory network motifs consisting of FFLs typically involve TFs, miRNAs and joint targets. Surveying possible instances of miRNA–mRNA–TF loops in our integrated time-lagged data sets allowed for identification of several FFLs that only became fully active at specific time points (Figure 7). Five temporally interconnected FFLs appeared to be of special interest because they could control the expression of genes involved in biological functions that are relevant to our model (cell adhesion, apoptosis and/or immune response or cell cycle). At 24 h, expression of ICAM-1 (intercellular adhesion molecule-1) gene appeared to be fine-tuned by a complex interplay between miR-21 and RelA itself under the control of miR-193b. Simultaneously, the expression of the BCL-2 protein family member MCL1 (myeloid cell leukemia sequence 1) gene was controlled by miR-29 and two TFs, the RelA/NF-κB complex and TP53. At 48 h, although the RelA/NF-κB TF complex was no longer active, TP53 still seemed to be involved in the miR-29–MCL1 loop, but also controlled the expression of let-7a-5p miRNA and BCL2L1 (BCL-2 like-1) gene, another member of the BCL-2 protein family. Finally, at 72 h, an FFL involving let-7a-5p miRNA and KDM5B [lysine (K)-specific demethylase 5B] TR appeared to modulate the expression of CCND1 (cyclin D1) gene. No active FFL were detected at 3, 12 and 72 h or in control

Figure 6. Circos diagrams showing dynamical dependency of the transcriptome, represented in the form of top biological categories (purple) and of inferred upstream regulators: transcription regulators (TRs: brown) and miRNAs (blue). Time points for 3, 12, 24, 48 and 72 h and for the 72-h JII-treated control were compared with the untreated control, and the SDE molecules were analysed by 'limma', with contrasts (FDR < 0.001) as described in 'Materials and Methods' section. The width of the categories is related to the number of member mRNAs. A connection between a TR and a functional category means that this TF was detected as an activated or inhibited TR by upstream regulator analysis, and that its target genes grouping in the respective functional category were differentially expressed in at least one time point. A connection between a miRNA and a TR implies that this miRNA was SDE and was predicted to target the TR genes. Finally, a connection between a miRNA and a functional category indicates that one or several of its target genes of a differentially expressed miRNA belonged to the assigned category. The thickness of connecting lines illustrates higher number of targets of TRs or miRNAs within this functional category.

Figure 7. Graphical representation of regulatory sub-networks (extracted from IPA) includes three activated TRs (dark grey boxes), four genes (rounded boxes) and four miRNAs (ellipses). Activation time for each part of the sub-network is shown by arrows on top. 'mir' represents the immature form of miRNAs, whereas 'miR' denotes the mature form. Connections between molecules are presented with respect to experimental observations and IPA predictions. Black: molecules have correlated (anti-correlated in case of inhibition) expression profiles. Dotted arrows: mRNA profile of a target molecule is in concordance with the predicted activation state of the TF. Grey arrows: direct interaction was not observed, suggesting presence of cumulative effect of other regulators.

samples treated with JII. Our data suggest that response to IFN-γ in our cell model involves a discrete set of TRs that act sequentially and/or synergistically on cell stimulation.

Taken together, the integrative analysis of data sets representing high-resolution time-series–derived mRNA and miRNA microarray data allowed us to detect dynamic interactions that would have been missed if only single time points were considered. Our biostatistical and bioinformatics analysis pipeline identified a very interesting time delay of the miRNome with respect to the transcriptome, and we speculate that most miRNAs become up-regulated only after the first round of transcriptional activation is completed. Furthermore, the incorporation of inferred biological functions added another level of complexity to this study, allowing for visualization of dynamic changes in functional systems.

DISCUSSION

Owing to their ability to post-transcriptionally regulate gene expression of almost all genes, miRNAs are known to influence many cellular activities in healthy and diseased states. Because they are involved in key cellular processes, it remains essential to decipher more miRNA target genes and to examine how miRNAs are regulated, their temporal dynamic behaviour and their involvement in defined cellular functions.

The current study was motivated by the question of how the functional interplay between mRNAs and miRNAs is regulated and changing dynamically. To explore the global temporal response to IFN-γ treatment, we examined the expression levels of miRNAs and mRNAs in a time-series experiment using A375 melanoma cells. Time-series analysis, as opposed to comparison of multiple steady states, gives important insights into the causality of the observed interactions: while normally only connections between molecules are described, time-series data allow for addressing the direction of the interaction and its rate, and thus provide a better understanding of cell dynamics (30,59). In a previous study (40),

we performed a detailed investigation of the dynamic behaviour of miRNAs over a wide time range after cytokine stimulation with IFN-γ, which activates the TF STAT1. A surprising finding of this former study was that all miRNA expression changes occurred with a delay only after 24 h. To find an explanation for this result and to identify dynamic regulatory networks, we performed a series of mRNA microarrays using the same RNA extracts. In addition to the identification of significantly regulated miRNAs and mRNAs over time, this approach allows for building and testing contrasts using the same linear model (45). Based on our benchmarking results of three methods ('betr', 'timecourse' and 'limma'), 'limma' proved to be superior in terms of FDR for permuted data sets and synthetic data. Using the 'limma' tool, we confirmed the previously reported 23 differentially regulated miRNAs (40), and further refined this data by detecting an additional 42 miRNAs with an FDR < 0.001 (Figure 3B).

Numbers of SDE genes and miRNAs (Figure 2B) and the heat maps (Figure 3) clearly revealed a delayed response of the miRNome to IFN-γ stimulation with respect to the transcriptome. Interestingly, Pedersen *et al.* (60) have described two miRNAs that were modulated already after 30 min after IFN-β stimulation of hepatocyte cells. Also, Kutty *et al.* (61) observed early regulation of miR-155 after exposure to a tumour necrosis factor-α, interleukin-1β and IFN-γ cytokine mixture. Here, we did not identify statistically significantly regulated mature miRNAs reacting that quickly to IFN-γ in melanoma cells. In this context, we have recently confirmed that primary miRNA transcripts (pri-miRNAs) and precursor form (pre-miRNAs) (of the miR-29 family) are up-regulated well before the corresponding mature miRNAs after IFN-γ stimulation of melanoma cells (62). The combined analysis of miRNA and mRNA data sets suggests that the IFN-γ–initiated Jak/STAT signalling cascade transcriptionally activates other downstream TFs as well as other effector genes, which may in turn participate in up-regulation of

expression levels of a number of responding miRNAs in melanoma cells.

On comparison of both data sets, we observed only three negatively regulated mRNAs at 3 h, while 117, including STAT1-3, IRF1-6, IFI16 and other IFN-λ-related genes, were up-regulated. From 24 h onwards, more down-regulated mRNAs were scored, which chronologically was in good concordance with the elevated miRNA levels, indicating that there might be an inverse correlation for some of these miRNA–mRNA pairs. Three main dynamic profiles were detected among the top 100 mRNAs (Figure 3A): late expression, early expression followed by repression and late repression. These profiles were also seen when analysing the expression profiles of all significant mRNA (Supplementary Figure S3). The 65 SDE miRNAs, in contrast, presented only two major dynamic profiles (Figure 3B): delayed up-regulation and delayed down-regulation similar to our previous results, which included a more detailed analysis of temporal miRNA profiles (40).

It is well accepted that identification of target mRNAs regulated by miRNAs is required to elucidate the exact role of individual miRNAs or groups of related miRNAs in a given cell. Several algorithms have been established for *in silico* predictions of target mRNAs [see review (25)]. However and as mentioned before, there is no efficient algorithm that reliably predicts all targets with a minimal number of false positives. A straight-forward approach to improve target gene predictions could be global correlation analyses of miRNAs and experimentally matched mRNA expression patterns in combination with standard target gene prediction algorithms at least for those interacting pairs where miRNAs cause a measureable decrease in mRNA levels. For this, we used the in-house–developed tool CoExpress to build a miRNA–mRNA correlation map, to compare negatively correlated miRNA–mRNA pairs with TargetScan predictions and to experimentally confirm interactions extracted from TarBase. Using this approach, we detected 398 negatively correlated predicted targets for 21 miRNAs (Supplementary Table S3 based on TargetScan), and we were able to validate 14 selected miRNA–mRNA pairs by qPCR (Supplementary Figure S5).

Overall, integrating time-series miRNA and mRNA data sets provides valuable information not only for identification of possible miRNA target genes but also for the elucidation of dynamic changes of the underlying biological processes. Using Circos plots, we visualized specific interactions between upstream TRs, miRNAs and also mRNAs that were categorized in a set of biological functions (Figure 6). Circos facilitates the integration of different data sets, thus providing a more holistic view of the evolving processes. Ebert and Sharp have recently summarized evidence that suggests miRNAs to actively confer robustness to biological processes by dampening and/or increasing cellular responses to internal or external stimuli (24). This random noise in transcription rates, and as such in expression levels of genes and proteins, may in part be kept within certain boundaries by the action of miRNAs. Our data on temporal expression changes within the miRNome and transcriptome as well as on TRs support this notion: in response to an external stimulus (IFN-γ), many TRs and other mRNAs react rapidly with measurable expression level changes, whereas miRNAs react with a considerable time delay. This tentative 'second wave' of responses then brings up-regulated miRNAs into play, which mostly down-regulate their respective target genes, and thus control and reduce inordinate cellular reactions.

Several interactions in the form of negative or positive FFLs have already been established between TFs and miRNAs (7,19,63). Very recently, Gerstein and collaborators described a comprehensive architecture of the human transcriptional regulatory meta-network derived from integrating data from the Encyclopedia of DNA Elements project with genomic and protein information (64). The authors found that this meta-network exhibited a high enrichment in FFLs, showing the importance of this motif in transcriptional regulatory process. Looking for specific FFLs, which include TFs regulating the expression of both a miRNA and its target mRNA at the same time (FFL type: 'miR → TF–targets', with edge from both regulators to target), we found several regulatory relationships that could be of interest in our biological system. By combining time-series stimulation of gene expression by TFs with delayed transcriptional repression by miRNAs, FFL motifs may create a toggle-switch mechanism by which the cell could timely coordinate responses to IFN-γ stimulation. Chalancon *et al.* (20) recently stated that to gain a better understanding of gene regulatory events in response to environmental changes, it is necessary to measure expression changes at highest possible resolution and under many different conditions over wider time ranges. Although our study describes a relatively small number of matched data sets, it represents the first attempt to move to more quantitative time-resolved data and could be considered as a proof of principle for more extensive studies in future incorporating more conditions, time points and cell systems; the herein established computational analysis pipeline can easily be adapted to additional data sources or requirements. Knowledge from integrated data on individual miRNAs, families of miRNAs and eventually on the entire miRNome together with dynamic and matched transcriptome data will contribute to a more comprehensive view of biological systems, their regulation and their behaviour over time.

SUPPLEMENTARY DATA

Supplementary Data are available at NAR Online: Supplementary Tables 1–3, Supplementary Figures 1–5, Supplementary Methods and Supplementary References [3,33,40,44–47,65–69].

ACKNOWLEDGEMENTS

FUNDING

REFERENCES

1. Lee,R.C., Feinbaum,R.L. and Ambros,V. (1993) The C. elegans heterochronic gene lin-4 encodes small RNAs with antisense complementarity to lin-14. *Cell*, **75**, 843–854.
2. He,L. and Hannon,G.J. (2004) MicroRNAs: small RNAs with a big role in gene regulation. *Nat. Rev. Genet.*, **5**, 522–531.
3. Friedman,R.C., Farh,K.K., Burge,C.B. and Bartel,D.P. (2009) Most mammalian mRNAs are conserved targets of microRNAs. *Genome Res.*, **19**, 92–105.
4. Mack,G.S. (2007) MicroRNA gets down to business. *Nat. Biotechnol.*, **25**, 631–638.
5. Bartel,D.P. (2004) MicroRNAs: genomics, biogenesis, mechanism, and function. *Cell*, **116**, 281–297.
6. Grosshans,H. and Filipowicz,W. (2008) Molecular biology: the expanding world of small RNAs. *Nature*, **451**, 414–416.
7. Krol,J., Loedige,I. and Filipowicz,W. (2010) The widespread regulation of microRNA biogenesis, function and decay. *Nat. Rev. Genet.*, **11**, 597–610.
8. Iorio,M.V. and Croce,C.M. (2012) microRNA involvement in human cancer. *Carcinogenesis*, **33**, 1126–1133.
9. Esquela-Kerscher,A. and Slack,F.J. (2006) Oncomirs - microRNAs with a role in cancer. *Nat. Rev. Cancer*, **6**, 259–269.
10. Ma,L. and Weinberg,R.A. (2008) MicroRNAs in malignant progression. *Cell Cycle*, **7**, 570–572.
11. Volinia,S., Calin,G.A., Liu,C.G., Ambs,S., Cimmino,A., Petrocca,F., Visone,R., Iorio,M., Roldo,C., Ferracin,M. *et al.* (2006) A microRNA expression signature of human solid tumors defines cancer gene targets. *Proc. Natl Acad. Sci. USA*, **103**, 2257–2261.
12. Calin,G.A. and Croce,C.M. (2006) MicroRNA signatures in human cancers. *Nat. Rev. Cancer*, **6**, 857–866.
13. Bartels,C.L. and Tsongalis,G.J. (2009) MicroRNAs: novel biomarkers for human cancer. *Clin. Chem.*, **55**, 623–631.
14. Sand,M., Gambichler,T., Sand,D., Skrygan,M., Altmeyer,P. and Bechara,F.G. (2009) MicroRNAs and the skin: tiny players in the body's largest organ. *J. Dermatol. Sci.*, **53**, 169–175.
15. Kasinski,A.L. and Slack,F.J. (2011) MicroRNAs en route to the clinic: progress in validating and targeting microRNAs for cancer therapy. *Nat. Rev. Cancer*, **11**, 849–864.
16. Morozova,N., Zinovyev,A., Nonne,N., Pritchard,L.L., Gorban,A.N. and Harel-Bellan,A. (2012) Kinetic signatures of microRNA modes of action. *RNA*, **18**, 1635–1655.
17. Wang,G., Wang,Y., Teng,M., Zhang,D., Li,L. and Liu,Y. (2010) Signal transducers and activators of transcription-1 (STAT1) regulates microRNA transcription in interferon gamma-stimulated HeLa cells. *PLoS One*, **5**, e11794.
18. Winter,J., Jung,S., Keller,S., Gregory,R.I. and Diederichs,S. (2009) Many roads to maturity: microRNA biogenesis pathways and their regulation. *Nat. Cell Biol.*, **11**, 228–234.
19. Yan,Z., Shah,P.K., Amin,S.B., Samur,M.K., Huang,N., Wang,X., Misra,V., Ji,H., Gabuzda,D. and Li,C. (2012) Integrative analysis of gene and miRNA expression profiles with transcription factor-miRNA feed-forward loops identifies regulators in human cancers. *Nucleic Acids Res.*, **40**, e135.
20. Chalancon,G., Ravarani,C.N., Balaji,S., Martinez-Arias,A., Aravind,L., Jothi,R. and Babu,M.M. (2012) Interplay between gene expression noise and regulatory network architecture. *Trends Genet.*, **28**, 221–232.
21. Turner,M. (2011) Is transcription the dominant force during dynamic changes in gene expression? *Adv Exp. Med. Biol.*, **780**, 1–13.
22. Lowrey,P.L. and Takahashi,J.S. (2011) Genetics of circadian rhythms in Mammalian model organisms. *Adv. Genet.*, **74**, 175–230.
23. Dougherty,E.R., Shmulevich,I. and Bittner,M.L. (2004) Genomic signal processing: the salient issues. *EURASIP J. Appl. Signal Process.*, **2004**, 146–153.
24. Ebert,M.S. and Sharp,P.A. (2012) Roles for microRNAs in conferring robustness to biological processes. *Cell*, **149**, 515–524.
25. Muniategui,A., Pey,J., Planes,F.J. and Rubio,A. (2012) Joint analysis of miRNA and mRNA expression data. *Brief. Bioinform.*, **1**, July 31 (doi: 10.1093/bib/bbs028; epub ahead of print).
26. Port,J.D., Walker,L.A., Polk,J., Nunley,K., Buttrick,P.M. and Sucharov,C.C. (2011) Temporal expression of miRNAs and mRNAs in a mouse model of myocardial infarction. *Physiol. Genomics*, **43**, 1087–1095.
27. Kim,Y., Kim,T.K., Kim,Y., Yoo,J., You,S., Lee,I., Carlson,G., Hood,L., Choi,S. and Hwang,D. (2011) Principal network analysis: identification of subnetworks representing major dynamics using gene expression data. *Bioinformatics*, **27**, 391–398.
28. Jayaswal,V., Lutherborrow,M., Ma,D.D. and Hwa Yang,Y. (2009) Identification of microRNAs with regulatory potential using a matched microRNA-mRNA time-course data. *Nucleic Acids Res.*, **37**, e60.
29. Schmeier,S., MacPherson,C.R., Essack,M., Kaur,M., Schaefer,U., Suzuki,H., Hayashizaki,Y. and Bajic,V.B. (2009) Deciphering the transcriptional circuitry of microRNA genes expressed during human monocytic differentiation. *BMC Genomics*, **10**, 595.
30. Bar-Joseph,Z., Gitter,A. and Simon,I. (2012) Studying and modelling dynamic biological processes using time-series gene expression data. *Nat. Rev. Genet.*, **13**, 552–564.
31. Kortylewski,M., Komyod,W., Kauffmann,M.E., Bosserhoff,A., Heinrich,P.C. and Behrmann,I. (2004) Interferon-gamma-mediated growth regulation of melanoma cells: involvement of STAT1-dependent and STAT1-independent signals. *J. Invest. Dermatol.*, **122**, 414–422.
32. Kakuta,S., Tagawa,Y., Shibata,S., Nanno,M. and Iwakura,Y. (2002) Inhibition of B16 melanoma experimental metastasis by interferon-gamma through direct inhibition of cell proliferation and activation of antitumour host mechanisms. *Immunology*, **105**, 92–100.
33. Smyth,G.K. (2004) Linear models and empirical bayes methods for assessing differential expression in microarray experiments. *Stat. Appl. Genet. Mol. Biol.*, **3**, Article 3.
34. Krzywinski,M., Schein,J., Birol,I., Connors,J., Gascoyne,R., Horsman,D., Jones,S.J. and Marra,M.A. (2009) Circos: an information aesthetic for comparative genomics. *Genome Res.*, **19**, 1639–1645.
35. Iliopoulos,D., Jaeger,S.A., Hirsch,H.A., Bulyk,M.L. and Struhl,K. (2010) STAT3 activation of miR-21 and miR-181b-1 via PTEN and CYLD are part of the epigenetic switch linking inflammation to cancer. *Mol. Cell*, **39**, 493–506.
36. Haghikia,A., Missol-Kolka,E., Tsikas,D., Venturini,L., Brundiers,S., Castoldi,M., Muckenthaler,M.U., Eder,M., Stapel,B., Thum,T. *et al.* (2011) Signal transducer and activator of transcription 3-mediated regulation of miR-199a-5p links cardiomyocyte and endothelial cell function in the heart: a key role for ubiquitin-conjugating enzymes. *Eur. Heart J.*, **32**, 1287–1297.
37. Brivanlou,A.H. and Darnell,J.E. Jr (2002) Signal transduction and the control of gene expression. *Science*, **295**, 813–818.
38. Levy,D.E. and Darnell,J.E. Jr (2002) Stats: transcriptional control and biological impact. *Nat. Rev. Mol. Cell Biol.*, **3**, 651–662.
39. Platanias,L.C. (2005) Mechanisms of type-I- and type-II-interferon-mediated signalling. *Nat. Rev. Immunol.*, **5**, 375–386.
40. Reinsbach,S.E., Nazarov,P.V., Philippidou,D., Schmitt,M., Wienecke-Baldacchino,A., Muller,A., Vallar,L., Behrmann,I. and Kreis,S. (2012) Dynamic regulation of microRNA expression following Interferon-γ-induced gene transcription. *RNA Biol.*, **9**, 1–12.

41. Gantier,M.P., McCoy,C.E., Rusinova,I., Saulep,D., Wang,D., Xu,D., Irving,A.T., Behlke,M.A., Hertzog,P.J., Mackay,F. *et al.* (2011) Analysis of microRNA turnover in mammalian cells following Dicer1 ablation. *Nucleic Acids Res.*, **39**, 5692–5703.

42. Irizarry,R.A., Hobbs,B., Collin,F., Beazer-Barclay,Y.D., Antonellis,K.J., Scherf,U. and Speed,T.P. (2003) Exploration, normalization, and summaries of high density oligonucleotide array probe level data. *Biostatistics*, **4**, 249–264.

43. Ayree,M.J. (2010) betr: Identify differentially expressed genes in microarray time-course data, R package, version 1.12.0, http://www.bioconductor.org.

44. Tai,Y.C. (2007) timecourse: Statistical Analysis for Developmental Microarray Time Course Data, R package, version 1.28.0, http://www.bioconductor.org.

45. Gillespie,C.S., Lei,G., Boys,R.J., Greenall,A. and Wilkinson,D.J. (2010) Analysing time course microarray data using Bioconductor: a case study using yeast2 Affymetrix arrays. *BMC Res. Notes*, **3**, 81.

46. Simpson,T.I., Armstrong,J.D. and Jarman,A.P. (2010) Merged consensus clustering to assess and improve class discovery with microarray data. *BMC Bioinformatics*, **11**, 590.

47. Vergoulis,T., Vlachos,I.S., Alexiou,P., Georgakilas,G., Maragkakis,M., Reczko,M., Gerangelos,S., Koziris,N., Dalamagas,T. and Hatzigeorgiou,A.G. (2012) TarBase 6.0: capturing the exponential growth of miRNA targets with experimental support. *Nucleic Acids Res.*, **40**, D222–D229.

48. Tsang,J., Zhu,J. and van Oudenaarden,A. (2007) MicroRNA-mediated feedback and feedforward loops are recurrent network motifs in mammals. *Mol. Cell*, **26**, 753–767.

49. Saha,B., Jyothi Prasanna,S., Chandrasekar,B. and Nandi,D. (2010) Gene modulation and immunoregulatory roles of interferon gamma. *Cytokine*, **50**, 1–14.

50. Jeffs,A.R., Glover,A.C., Slobbe,L.J., Wang,L., He,S., Hazlett,J.A., Awasthi,A., Woolley,A.G., Marshall,E.S., Joseph,W.R. *et al.* (2009) A gene expression signature of invasive potential in metastatic melanoma cells. *PLoS One*, **4**, e8461.

51. Harris,M.L., Baxter,L.L., Loftus,S.K. and Pavan,W.J. (2010) Sox proteins in melanocyte development and melanoma. *Pigment Cell Melanoma Res.*, **23**, 496–513.

52. Liu,H., Wei,Q., Gershenwald,J.E., Prieto,V.G., Lee,J.E., Duvic,M., Grimm,E.A. and Wang,L.E. (2012) Influence of single nucleotide polymorphisms in the MMP1 promoter region on cutaneous melanoma progression. *Melanoma Res.*, **22**, 169–175.

53. Landreville,S., Agapova,O.A., Matatall,K.A., Kneass,Z.T., Onken,M.D., Lee,R.S., Bowcock,A.M. and Harbour,J.W. (2012) Histone deacetylase inhibitors induce growth arrest and differentiation in uveal melanoma. *Clin. Cancer Res.*, **18**, 408–416.

54. Lehtonen,A., Matikainen,S. and Julkunen,I. (1997) Interferons up-regulate STAT1, STAT2, and IRF family transcription factor gene expression in human peripheral blood mononuclear cells and macrophages. *J. Immunol.*, **159**, 794–803.

55. Forbes,S.A., Tang,G., Bindal,N., Bamford,S., Dawson,E., Cole,C., Kok,C.Y., Jia,M., Ewing,R., Menzies,A. *et al.* (2010) COSMIC (the Catalogue of Somatic Mutations in Cancer): a resource to investigate acquired mutations in human cancer. *Nucleic Acids Res.*, **38**, D652–D657.

56. Clark,M.J., Homer,N., O'Connor,B.D., Chen,Z., Eskin,A., Lee,H., Merriman,B. and Nelson,S.F. (2010) U87MG decoded: the genomic sequence of a cytogenetically aberrant human cancer cell line. *PLoS Genet.*, **6**, e1000832.

57. Lucker,S., Wagner,M., Maixner,F., Pelletier,E., Koch,H., Vacherie,B., Rattei,T., Damste,J.S., Spieck,E., Le Paslier,D. *et al.* (2010) A Nitrospira metagenome illuminates the physiology and evolution of globally important nitrite-oxidizing bacteria. *Proc. Natl Acad. Sci. USA*, **107**, 13479–13484.

58. Neph,S., Stergachis,A.B., Reynolds,A., Sandstrom,R., Borenstein,E. and Stamatoyannopoulos,J.A. (2012) Circuitry and dynamics of human transcription factor regulatory networks. *Cell*, **150**, 1274–1286.

59. Gao,S., Hartman,J.L. IV, Carter,J.L., Hessner,M.J. and Wang,X. (2010) Global analysis of phase locking in gene expression during cell cycle: the potential in network modeling. *BMC Syst. Biol.*, **4**, 167.

60. Pedersen,I.M., Cheng,G., Wieland,S., Volinia,S., Croce,C.M., Chisari,F.V. and David,M. (2007) Interferon modulation of cellular microRNAs as an antiviral mechanism. *Nature*, **449**, 919–922.

61. Kutty,R.K., Nagineni,C.N., Samuel,W., Vijayasarathy,C., Hooks,J.J. and Redmond,T.M. (2010) Inflammatory cytokines regulate microRNA-155 expression in human retinal pigment epithelial cells by activating JAK/STAT pathway. *Biochem. Biophys. Res. Commun.*, **402**, 390–395.

62. Schmitt,M.J., Philippidou,D., Reinsbach,S.E., Margue,C., Wienecke-Baldacchino,A., Nashan,D., Behrmann,I. and Kreis,S. (2012) Interferon-gamma-induced activation of Signal Transducer and Activator of Transcription 1 (STAT1) up-regulates the tumor suppressing microRNA-29 family in melanoma cells. *Cell communication and signaling : CCS*, **10**, 41.

63. Sun,J., Gong,X., Purow,B. and Zhao,Z. (2012) Uncovering MicroRNA and transcription factor mediated regulatory networks in glioblastoma. *PLoS Comput. Biol.*, **8**, e1002488.

64. Gerstein,M.B., Kundaje,A., Hariharan,M., Landt,S.G., Yan,K.K., Cheng,C., Mu,X.J., Khurana,E., Rozowsky,J., Alexander,R. *et al.* (2012) Architecture of the human regulatory network derived from ENCODE data. *Nature*, **489**, 91–100.

65. Philippidou,D., Schmitt,M., Moser,D., Margue,C., Nazarov,P.V., Muller,A., Vallar,L., Nashan,D., Behrmann,I. and Kreis,S. (2010) Signatures of microRNAs and selected microRNA target genes in human melanoma. *Cancer Res*, **70**, 4163–4173.

66. Vandesompele,J., De Preter,K., Pattyn,F., Poppe,B., Van Roy,N., De Paepe,A. and Speleman,F. (2002) Accurate normalization of real-time quantitative RT-PCR data by geometric averaging of multiple internal control genes. *Genome Biol.*, **3**, 1–12.

67. Aryee,M.J., Gutierrez-Pabello,J.A., Kramnik,I., Maiti,T. and Quackenbush,J. (2009) An improved empirical bayes approach to estimating differential gene expression in microarray time-course data: BETR (Bayesian Estimation of Temporal Regulation). *BMC Bioinformatics*, **10**, 409.

68. Nepomuceno-Chamorro,I., Azuaje,F., Devaux,Y., Nazarov,P.V., Muller,A., Aguilar-Ruiz,J.S. and Wagner,D.R. (2011) Prognostic transcriptional association networks: a new supervised approach based on regression trees. *Bioinformatics*, **27**, 252–258.

69. Moussay,E., Wang,K., Cho,J.H., van Moer,K., Pierson,S., Paggetti,J., Nazarov,P.V., Palissot,V., Hood,L.E., Berchem,G. *et al.* (2011) MicroRNA as biomarkers and regulators in B-cell chronic lymphocytic leukemia. *Proc. Natl Acad. Sci. USA*, **108**, 6573–6578.